Heliyon 10 (2024) e34713

Contents lists available at ScienceDirect

Heliyon

journal homepage: www.cell.com/heliyon

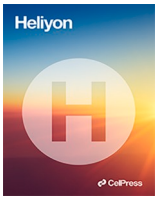

Research article

Exploring *Bryophyllum pinnatum* compounds as potential inhibitors for *Vespula vulgaris* allergen proteins: A systematic computational approach

Sirajul Islam , Abu Zaffar Shibly *

Department of Biotechnology and Genetic Engineering, Mawlana Bhashani Science and Technology University, Tangail, Santosh, 1902, Bangladesh

A B S T R A C T

Vespula vulgaris (V. vulgaris), commonly known as the common wasp, poses a significant health threat due to its venom-induced allergic reactions. This research focused on the exploration of bioactive compounds from *Bryophyllum pinnatum* as potential inhibitors for *V. vulgaris* allergen proteins, including Phospholipase A1 (Ves V1), Hyaluronoglucosaminidase (Ves V2), and Antigen 5 (Ves V5). Through a multidisciplinary approach involving literature reviews, molecular docking analyses, ADMET assessments and Molecular Dynamics Simulations (MDS) of 100ns we identified two promising drug candidates from four bioactive compounds- Bryophyllin A, Bryophyllin B, Bryotoxin A, and Bryotoxin B of *Bryophyllum pinnatum*. Molecular docking results revealed strong binding interactions, with Bryophyllin B and Bryotoxin A consistently exhibiting the highest affinity (−9.6 kcal/mol and −10.0 kcal/mol) across the allergen proteins. ADMET analyses highlighted Bryophyllin B as a favorable candidate, showing high absorption (HIA: 92.1 %), minimal metabolic interactions (CYP1A2: No), and a low toxicity profile (LD_{50} (rat): 2.431). MDS analysis revealed Bryophyllin B and Bryotoxin A as promising drug inhibitors, exhibiting the highest binding stability with the allergen proteins of *V. vulgaris*, as indicated by the lowest Root Mean Square Deviation (RMSD), Root Mean Square Fluctuation (RMSF), Radius of Gyration (RG) values and highest protein-ligand contacts. Our study provides valuable insights into the therapeutic potential of *Bryophyllum pinnatum* compounds as inhibitors for *V. vulgaris* allergen proteins having two promising candidates- Bryophyllin B and Bryotoxin A.

1. Introduction

Vespula vulgaris (V. vulgaris), commonly known as the common wasp, poses a significant health threat due to its venom-induced allergic reactions in humans. The venom of *V. vulgaris* contains a complex mixture of bioactive compounds, including allergen proteins such as Phospholipase A1 (Ves V1), Hyaluronoglucosaminidase (Ves V2), and Antigen 5 (Ves V5) [1,2], which are known to trigger allergic responses in susceptible individuals [3–6]. These allergen proteins elicit a cascade of immunological reactions upon exposure, leading to various adverse effects ranging from localized swelling and itching to potentially life-threatening systemic reactions like anaphylactic shock [1,7,8].

The mechanism of allergic sensitization to wasp venom involves the recognition of these allergens by the immune system, leading to the production of specific immunoglobulin E (IgE) antibodies and subsequent activation of mast cells and basophils, resulting in the release of inflammatory mediators such as histamine and leukotrienes [9–12]. As the incidence of wasp venom allergies continues to rise globally, there is an urgent need to explore innovative therapeutic strategies to mitigate allergic reactions induced by *V. vulgaris* venom [13]. Traditional treatment options for wasp venom allergies include allergen-specific immunotherapy (desensitization) and symptomatic management with antihistamines, corticosteroids, and epinephrine for severe reactions [10,14–16,16]. However, these approaches have limitations, including the need for long-term treatment and potential adverse effects [17–20].

* Corresponding author. Dept of Biotechnology and Genetic Engineering, Bangladesh.
E-mail addresses: sirajulislamsiru255@gmail.com (S. Islam), zaffarshibly@mbstu.ac.bd (A.Z. Shibly).

https://doi.org/10.1016/j.heliyon.2024.e34713
Received 10 May 2024; Received in revised form 12 July 2024; Accepted 15 July 2024
Available online 22 July 2024

In this context, the exploration of natural compounds with potential inhibitory effects on *V. vulgaris* allergen proteins presents a promising avenue for novel therapeutic interventions. *Bryophyllum pinnatum*, a succulent plant with a rich history in traditional medicine, has emerged as a source of bioactive compounds with pharmacological properties, including anti-inflammatory and immunomodulatory effects. Through a comprehensive literature review, four bioactive compounds- Bryophyllin A, Bryophyllin B, Bryotoxin A, and Bryotoxin B - have been identified within *Bryophyllum pinnatum*, showing promising inhibitory effects against different allergen proteins.

This study aimed to delve into the molecular interactions between the identified bioactive compounds and *V. vulgaris* allergen proteins. Through molecular docking analyses and structural examinations, we sought to elucidate the binding mechanisms and potential inhibitory effects of *Bryophyllum pinnatum* compounds on the allergen proteins. The insights gained from this exploration could pave the way for the development of novel therapeutics to alleviate the allergic burden imposed by *V. vulgaris* venom. As we embarked on this investigation, it is important to underscore the urgency of finding effective interventions for wasp venom allergies and the potential of natural compounds from *Bryophyllum pinnatum* as promising candidates.

2. Materials and methods

2.1. Data retrieval

The allergen proteins of *V. vulgaris* were identified through a comprehensive literature review. Subsequently, their three-dimensional structures were obtained from the RCSB PDB server [21]. The active compounds from *Bryophyllum pinnatum* were selected based on literature highlighting their potential as inhibitors, particularly in the context of COVID-19 cytokine storm therapy [22–24]. The chemical structures of these compounds were retrieved in sdf format from the PubChem server (https://pubchem.ncbi.nlm.nih.gov/). This approach ensured a thorough and well-informed selection of both the target proteins and the active compounds, laying the foundation for subsequent molecular docking analyses to explore potential inhibitory interactions between *Bryophyllum pinnatum* compounds and *V. vulgaris* allergen proteins.

2.2. Molecular docking analysis

The allergen proteins of *V. vulgaris* (1QNX - Ves V5, 2ATM - Ves V2, and 4QNN - Ves V1) were prepared using the Discovery Studio tool, involving tasks such as energy minimization, removal of water molecules, and assignment of appropriate charges. Additionally, drug binding cavities of the allergen proteins were identified utilizing the CBDOCK2 online server. For the active compounds from *Bryophyllum pinnatum* (Bryophyllin A, Bryophyllin B, Bryotoxin A, and Bryotoxin B), similar preparations were performed using the Open Babel tool, involving energy minimization and structural refinement. The molecular docking analysis was executed using PyRx software, wherein the prepared compounds and allergen proteins were docked to predict their binding interactions [25]. The site-specific docking was performed, using the coordinates and dimensions of the cavities detected by the CBDOCK2 online server [26]. The molecular docking results were subsequently analyzed to assess the binding affinities and key interactions between the active compounds and the allergen proteins, providing valuable insights into the potential inhibitory effects of *Bryophyllum pinnatum* compounds on *V. vulgaris* allergens.

2.3. Molecular properties and ADMET analysis of the bioactive compounds

ADMET properties refer to the pharmacokinetic characteristics of a drug candidate, encompassing Absorption, Distribution, Metabolism, Excretion and Toxicity. These properties play a crucial role in determining the bioavailability, efficacy, and safety of a drug [27–30]. The molecular properties and ADMET analysis of the active compounds from *Bryophyllum pinnatum*, three online servers-pkCSM (Predicting the Activity and Specificity of Kinases using Molecular Signatures), SwissADME and Protox-II were employed. For molecular properties, the pkCSM and SwissADME servers were utilized to predict key physicochemical characteristics such as molecular weight, LogP, rotatable bonds, hydrogen bond acceptors and donors, surface area, Lipinski Rule of Five violations and ADME properties [31–34]. pkCSM provided insights into absorption (Caco-2 permeability and human intestinal absorption) [35], distribution (blood-brain barrier and central nervous system permeability), metabolism (CYP1A2 inhibition) [36], and excretion (total clearance). On the other hand, Protox-II contributed toxicity predictions including hepatotoxicity, mutagenicity, cytoxicity, carcinogenicity, and immunotoxicity [37,38]. The combined utilization of these servers enabled a comprehensive evaluation of the molecular properties and pharmacokinetic parameters of the compounds, offering valuable information for further assessment of their drug-likeness and safety profiles.

2.4. Molecular dynamics (MD) simulation of the protein-ligand complexes

Molecular dynamics (MD) simulations are commonly utilized to assess the stability of candidate drug compounds bound to target proteins [39–41]. In this study, we conducted MD simulations lasting 100 ns using the Desmond software package by Schrödinger LLC. Prior to simulation, preprocessing steps were applied to the protein-ligand complexes, including optimization and minimization, using either the Protein Preparation Wizard in Maestro software or the System Builder tool. The simulations were set up in an orthorhombic simulation box with TIP3P solvent model to mimic realistic environmental conditions [42]. OPLS_2005 force field was employed, and counter ions were added as necessary to neutralize the system [41]. To mimic physiological conditions, a 0.15 M salt solution (NaCl)

Table 01
Four bioactive compounds from *Bryophyllum pinnatum*.

Compounds	Pubchem ID	Formula	Canonical Smile
Bryophyllin A	5488801	$C_{26}H_{32}O_8$	CC12CC(C3C(C1(CCC2C4═COC(═O)C═C4)O)CCC56C3(C7CC(C5)OC(O7)(O6)C)C═O)O
Bryophyllin B	44575928	$C_{26}H_{34}O_9$	CC(═O)OC1CC(CC2(C13C4C(CC2)C5(CCC(C5(CC4OC3O)C)C6═COC(═O)C═C6)O)O)O
Bryotoxin A	441848	$C_{32}H_{42}O_{12}$	CC1CC(C(O1)OC2CCC3(C4C(CCC3(C2)O)C5(CCC(C5(C(═O)C4O)C)C6═COC(═O)C═C6)O)C═O)O)OC(═O)C
Bryotoxin B	5489391	$C_{26}H_{32}O_9$	CC12C(CCC1(C3CCC45CC6CC(C4(C3C(C2═O)O)CO)OC(O6)(O5)C)O)C7═COC(═O)C═C7

Table 02
Molecular Docking analysis.

Protein	Compound	Docking Score	CurPocket ID	Cavity Volume(Å^3)	Center (x, y, z)	Docking size (x, y, z)
1QNX (Ves V5)	Bryophyllin A	−8.4	C2	187	21, 31, 36	23, 23, 23
	Bryophyllin B	−9.6	C2	187	21, 31, 36	23, 23, 23
	Bryotoxin A	−8.3	C3	184	15, 25, 31	26, 26, 26
	Bryotoxin B	−8.3	C2	187	21, 31, 36	23, 23, 23
2ATM (Ves V2)	Bryophyllin A	−7.7	C1	504	19, 29, 8	23, 23, 23
	Bryophyllin B	−8.2	C1	504	19, 29, 8	23, 23, 23
	Bryotoxin A	−9.1	C1	504	19, 29, 8	26, 26, 26
	Bryotoxin B	−8.0	C1	504	19, 29, 8	23, 23, 23
4QNN (Ves V1)	Bryophyllin A	−9.9	C1	9257	−7, −7, 13	35, 33, 35
	Bryophyllin B	−9.4	C1	9257	−7, −7, 13	35, 33, 35
	Bryotoxin A	−10.0	C2	3809	−3, 15, −20	32, 26, 26
	Bryotoxin B	−9.0	C2	3809	−3, 15, −20	32, 23, 30

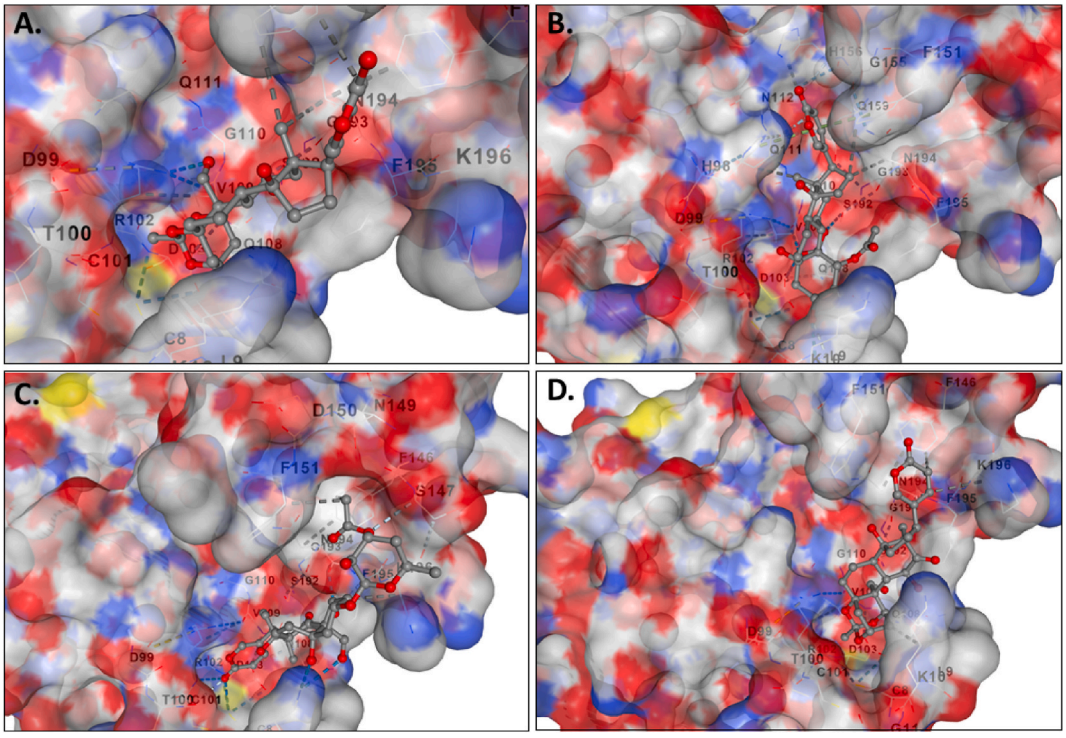

Fig. 1. The binding of compounds to the cavities of the allergen protein Antigen 5 (Ves V5) of *Vespula vulgaris*. Specifically, **A.** Bryophyllin A, **B.** Bryophyllin B, **C.** Bryotoxin A, and **D.** Bryotoxin B are shown binding in cavities C2, C2, C3, and C1, respectively.

was introduced. Throughout the simulation, equilibrium was maintained using NVT and NPT ensembles, with temperature and pressure held constant at 300 K and 1 atm, respectively, to conserve moles (N), pressure (P), and temperature (T). Pre-simulation relaxation procedures were conducted, and parameters such as radius of gyration (RG), solvent-accessible surface area (SASA), root mean square deviation (RMSD) [43], root mean square fluctuations (RMSF), and torsion angles [44] were computed to evaluate simulation stability for both the control and top four selected complexes.

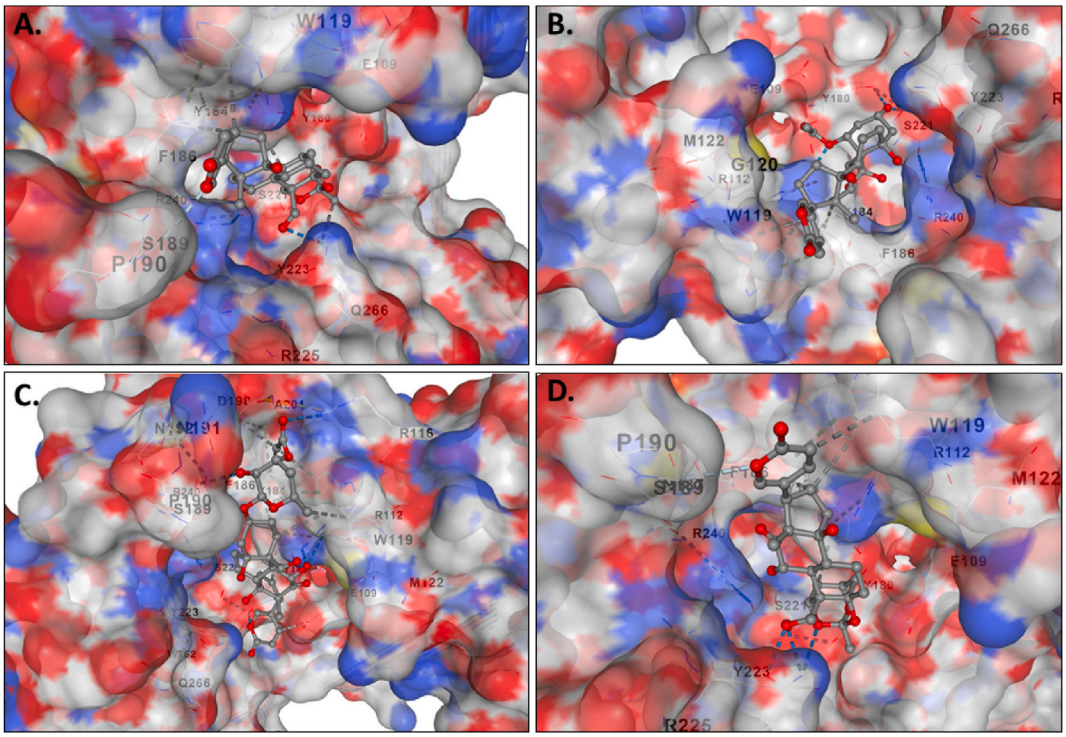

Fig. 2. The binding of compounds to the cavities of the allergen protein Hyaluronoglucosaminidase (Ves V2) of *Vespula vulgaris*. Specifically, **A.** Bryophyllin A, **B.** Bryophyllin B, **C.** Bryotoxin A, and **D.** Bryotoxin B are all shown binding in cavities C1.

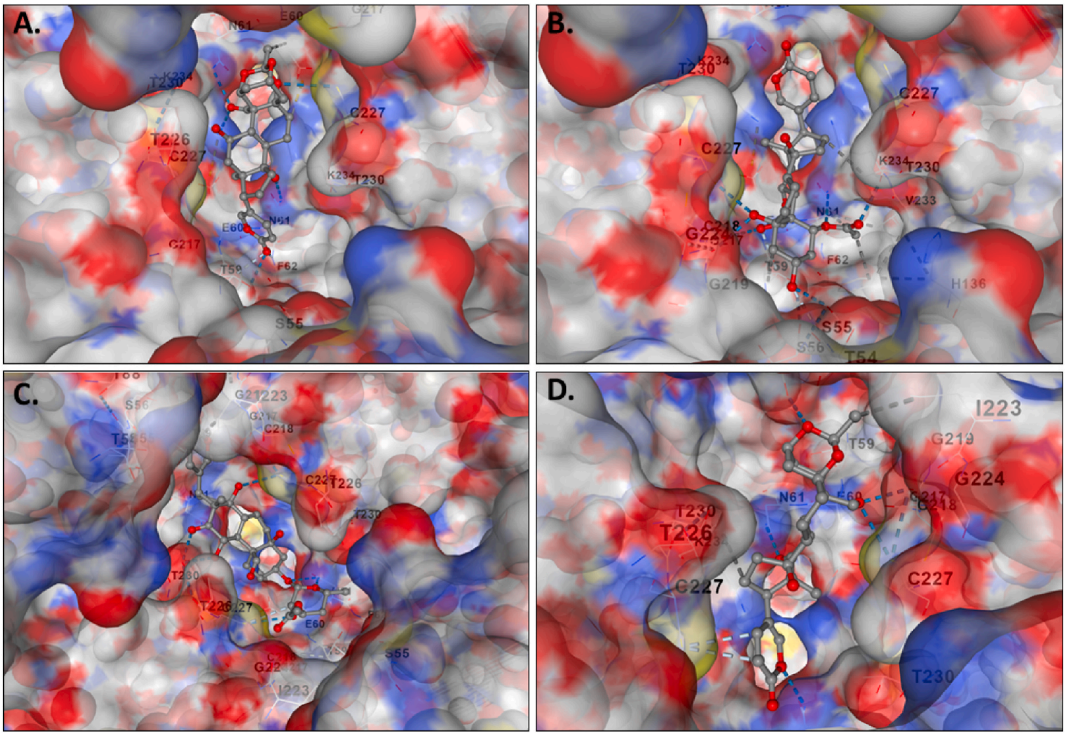

Fig. 3. The binding of compounds to the cavities of the allergen protein Phospholipase A1 (Ves V1) of *Vespula vulgaris*. Specifically, **A.** Bryophyllin A, **B.** Bryophyllin B, **C.** Bryotoxin A, and **D.** Bryotoxin B are shown binding in cavities C1, C1, C2 and C2 respectively.

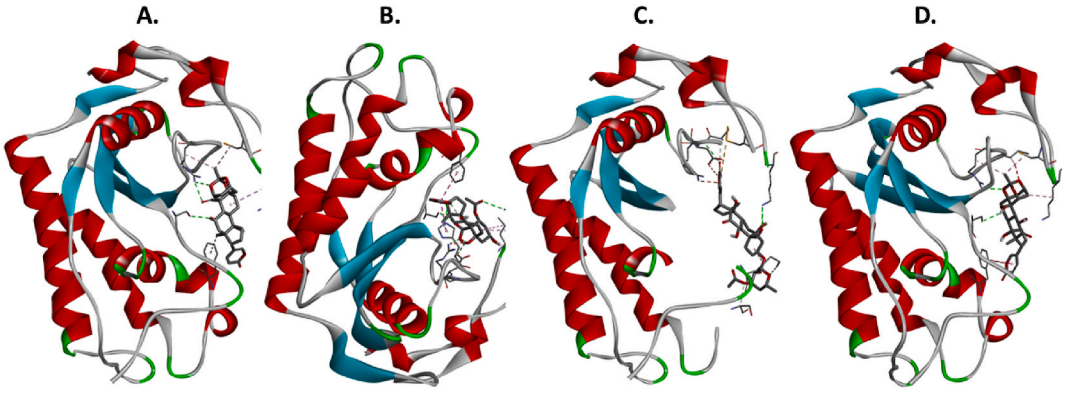

Fig. 4. Molecular docking: Binding of the four bioactive compounds- **A.** Bryophyllin A, **B.** Bryophyllin B, **C.** Bryotoxin A, and **D.** Bryotoxin B from *Bryophyllum pinnatum* with the allergen protein Antigen 5 (Ves V5) of *Vespula vulgaris*.

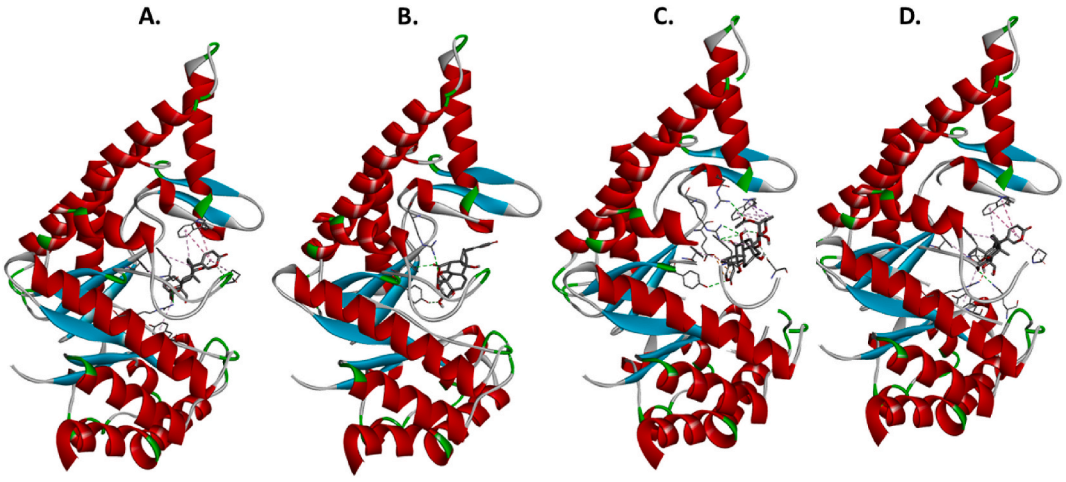

Fig. 5. Molecular docking: Binding of the four bioactive compounds- **A.** Bryophyllin A, **B.** Bryophyllin B, **C.** Bryotoxin A, and **D.** Bryotoxin B from *Bryophyllum pinnatum* with the allergen protein Hyaluronoglucosaminidase (Ves V2) of *Vespula vulgaris*.

3. Results and discussion

3.1. Data retrieval

Three allergen proteins from *V. vulgaris* were identified through a literature review: Phospholipase A1 (Ves V1), Hyaluronoglucosaminidase (Ves V2), and Antigen 5 (Ves V5). The 3D structures of these proteins were obtained from the RCSB PDB server, with PDB IDs 4QNN, 2ATM, and 1QNX, respectively. Specifically, 4QNN (Ves V1) consists of four chains (chain A, B, C, and D) and has a length of 300 amino acids. 2ATM (Ves V2) comprises a single chain (chain A) with a length of 331 amino acids, while 1QNX (Ves V5) consists of a single chain (chain A) and comprises 209 amino acid residues.

In addition, we identified four bioactive compounds within *Bryophyllum pinnatum* from literature review. They are Bryophyllin A, Bryophyllin B, Bryotoxin A, and Bryotoxin B [23]. The molecular structures of these compounds were retrieved from the PubChem server [45,46], with PubChem IDs 5488801, 44575928, 441848, and 5489391, respectively (Table 01).

3.2. Molecular docking analysis

The molecular docking results for the active compounds (Bryophyllin A, Bryophyllin B, Bryotoxin A, and Bryotoxin B) of *Bryophyllum pinnatum* with the allergic proteins of *V. vulgaris* demonstrated robust binding interactions [47]. Across proteins 1QNX (Ves V5), 2ATM (Ves V2), and 4QNN (Ves V1), all compounds consistently exhibited low docking scores, indicating strong binding affinities (Table 02). For 1QNX, Bryophyllin B displayed the highest affinity with a score of −9.6 kcal/mol, followed closely by Bryotoxin B with a score of −8.3 kcal/mol. In 2ATM, Bryotoxin A exhibited the highest affinity with a score of −9.1 kcal/mol. In 4QNN, Bryotoxin A again demonstrated the strongest binding with an impressive score of −10.0 kcal/mol. The identified binding pockets (Table S1), such

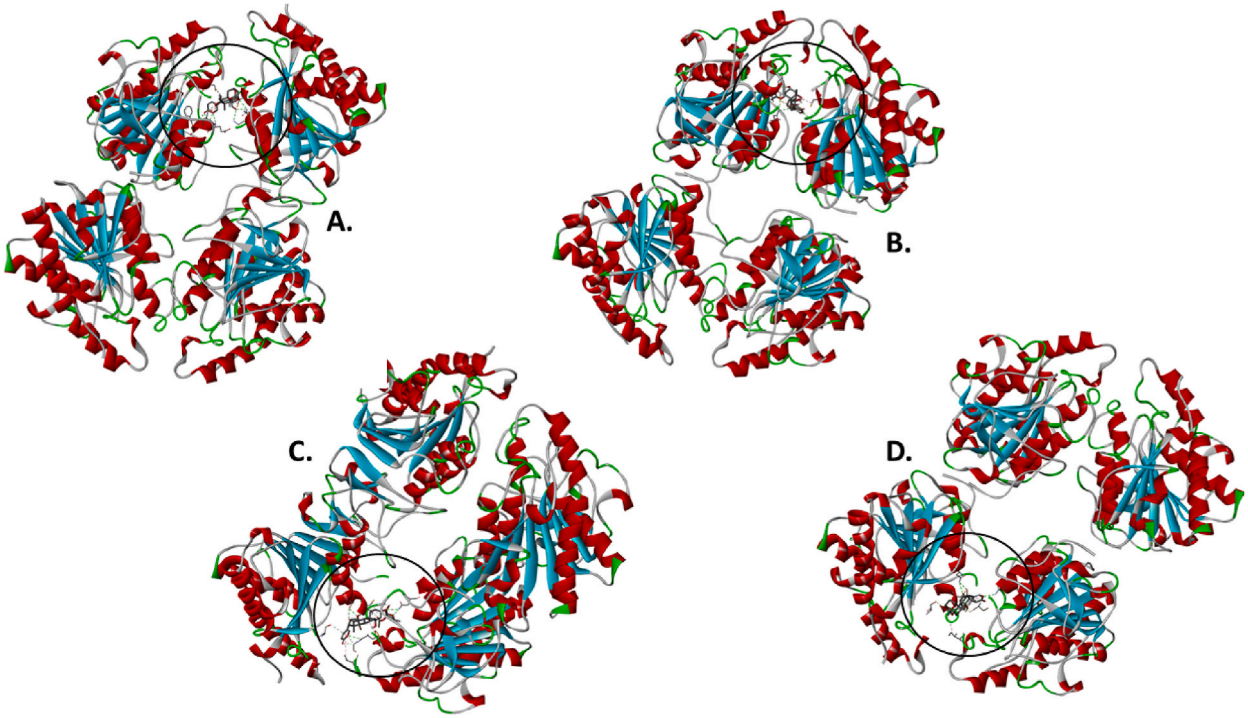

Fig. 6. Molecular docking: Binding of the four bioactive compounds- **A.** Bryophyllin A, **B.** Bryophyllin B, **C.** Bryotoxin A, and **D.** Bryotoxin B from *Bryophyllum pinnatum* with the allergen protein Phospholipase A1 (Ves V1) of *Vespula vulgaris*.

Table 03
Interacted amino acid residues of allergen proteins of *V. vulgaris* with bioactive compounds of *Bryophyllum pinnatum*.

Protein	Compound	Contact Residues
1QNX (Ves V5)	Bryophyllin A	**Chain A:** CYS8, LYS10, ARG102, PHE151, SER192
	Bryophyllin B	**Chain A:** LEU9, LYS10, HIS98, ARG102, ASP103, PHE151, SER192
	Bryotoxin A	**Chain A:** CYS8, LYS10, CYS101, ARG102, ASP103, SER147, LYS196
	Bryotoxin B	**Chain A:** CYS8, LYS10, THR100, ARG102, PHE151, SER192
2ATM (Ves V2)	Bryophyllin A	**Chain A:** TRP119, TYR184, PHE186, PRO190, TYR223, ARG240
	Bryophyllin B	**Chain A:** ARG112, TYR180, TYR184
	Bryotoxin A	**Chain A:** GLU109, ARG112, ARG116, TRP119, TYR180, TYR184, PHE186, SER189
	Bryotoxin B	**Chain A:** TRP119, TYR184, PHE186, PRO190, TYR223, ARG240, GLN266
4QNN (Ves V1)	Bryophyllin A	**Chain A:** ASN61, LYS234, CYS227
		Chain C: GLU60, ASN61, PHE62, CYS227
	Bryophyllin B	**Chain A:** ASN61, GLY217
		Chain C: SER55, ASN61, CYS227, THR230
	Bryotoxin A	**Chain B:** ASN61, CYS218, GLY219, ILE223, CYS227
		Chain D: SER55, GLY224, CYS227, THR230
	Bryotoxin B	**Chain B:** ASN61, CYS218, ILE223
		Chain D: SER55, ASN61, CYS227

as C2 in 1QNX, C1 in 2ATM, and C1 in 4QNN, were consistent among different proteins, indicating potential shared interaction sites (Fig. 1**(A–D)**, Fig. 2**(A–D)** and Fig. 3 **(A–D)**). Notably, Bryotoxin A consistently stood out as the compound with the highest binding fitness across all three proteins, suggesting its strong potential for interacting with the allergic proteins of *V. vulgaris*. The binding poses of protein-ligand complexes are demonstrated in Fig. 4**(A–D)**, Fig. 5**(A–D)** and Fig. 6**(A–D)**. The interacted amino acid residues (Table 03) and bond types are depicted in Fig. 7**(A–D)**, Fig. 8**(A–D)** and Fig. 9 **(A–D)**.

3.3. Molecular properties analysis

The molecular properties of the active compounds from *Bryophyllum pinnatum*, including Bryophyllin A, Bryophyllin B, Bryotoxin A, and Bryotoxin B, were analyzed to gauge their drug-likeness. Bryophyllin A and Bryophyllin B, with molecular weights of 472.534 g/mol and 490.549 g/mol, respectively, demonstrated moderate sizes within the desirable range. Both compounds exhibited favorable logP values around 1, indicative of a balanced hydrophilic-lipophilic profile for efficient drug absorption and distribution. With two

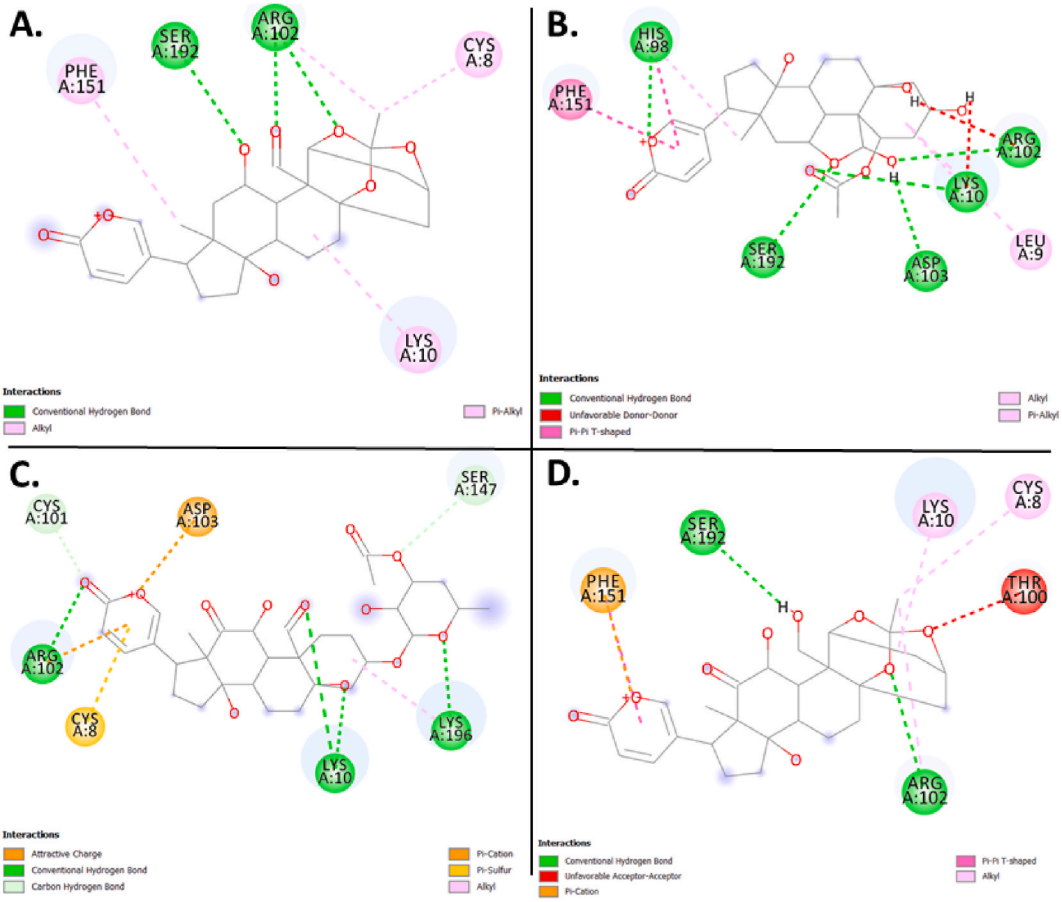

Fig. 7. Molecular docking: Binding interactions (Bond types) of the four bioactive compounds- **A.** Bryophyllin A, **B.** Bryophyllin B, **C.** Bryotoxin A, and **D.** Bryotoxin B from *Bryophyllum pinnatum* with the allergen protein Antigen 5 (Ves V5) of *Vespula vulgaris*.

rotatable bonds, Bryophyllin A and Bryophyllin B showcased reasonable flexibility. Bryotoxin A, characterized by a higher molecular weight of 618.676 and five rotatable bonds, and Bryotoxin B, with three, indicated a greater degree of molecular flexibility. The number of hydrogen bond acceptors (HBA) and donors (HBD) varied, with Bryotoxin A possessing higher values, suggesting potential for increased hydrogen bonding interactions. While all compounds adhered to Lipinski's rule of five, Bryotoxin A's two violations indicate a departure from conventional drug-like criteria. These molecular property assessments provide valuable insights into the compounds' pharmacokinetic characteristics, aiding in the evaluation of their potential as drug candidates (Table 04).

3.4. ADMET analysis

The ADMET analysis of the active compounds from *Bryophyllum pinnatum* provides valuable insights into their pharmacokinetic properties and potential therapeutic suitability [48–50]. Bryophyllin A and Bryophyllin B exhibited favorable absorption, as indicated by Caco-2 permeability (C2P) values of 1.351 and 0.57, respectively. Moreover, both compounds demonstrated high human intestinal absorption (HIA) percentages of 85.237 % and 92.164 %, respectively. Notably, Bryophyllin B showed the highest absorption, suggesting its potential as an orally bioavailable drug. The compounds exhibited negligible P-glycoprotein inhibition (P-gpI), indicating minimal impact on drug efflux. While Bryotoxin A and Bryotoxin B showed lower HIA percentages, Bryotoxin B displays excellent Caco-2 permeability. None of the compounds appeared to inhibit CYP1A2, reducing the likelihood of metabolic interactions. The blood-brain barrier (BBB) and central nervous system (CNS) permeability values suggested limited brain penetration for all compounds. Importantly, no hepatotoxicity was indicated, and the oral rat acute toxicity (LD50) values fallen within an acceptable range, with Bryotoxin B having the highest LD50 (Table 05).

The toxicity analysis provides crucial insights into their safety profiles and potential adverse effects. Bryophyllin A, Bryophyllin B, and Bryotoxin A shared a toxicity class of 2, with predicted LD50 values of 31 mg/kg, indicating moderate toxicity. In contrast, Bryophyllin B was classified in toxicity class 3, with a higher predicted LD50 of 144 mg/kg, suggesting a comparatively lower toxicity. Importantly, all compounds exhibited inactive hepatotoxicity, mutagenicity, and immunotoxicity, highlighting their favorable safety profiles in these aspects. However, cytoxicity was predicted to be active for Bryophyllin A, Bryophyllin B, and Bryotoxin A, suggesting a

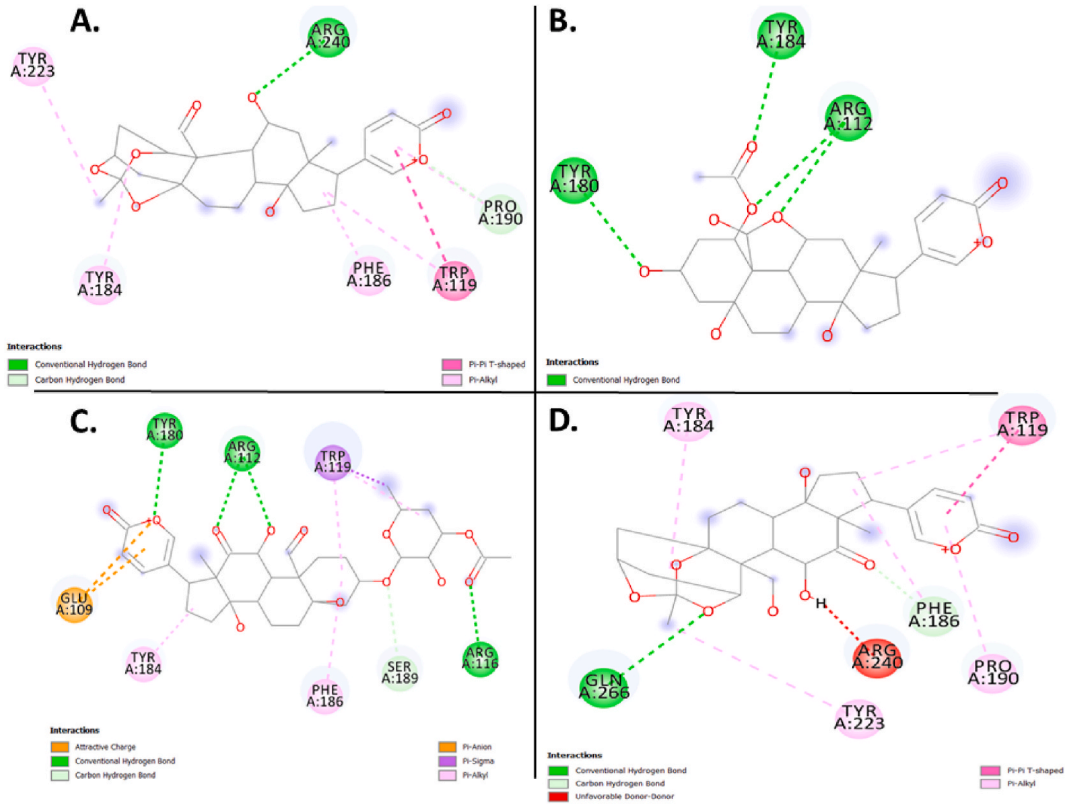

Fig. 8. Molecular docking: Binding interactions (Bond types) of the four bioactive compounds- **A.** Bryophyllin A, **B.** Bryophyllin B, **C.** Bryotoxin A, and **D.** Bryotoxin B from *Bryophyllum pinnatum* with the allergen protein Hyaluronoglucosaminidase (Ves V2) of *Vespula vulgaris*.

potential impact on cell viability. Carcinogenicity was predicted to be active for Bryophyllin A and Bryotoxin A, emphasizing the need for further investigation into their long-term effects (Table 06).

Overall, Bryophyllin B emerged as a promising candidate with high absorption, minimal metabolic interactions, and low toxicity profile, marked by lower predicted oral toxicity and the absence of predicted carcinogenicity.

3.5. Analysis of molecular dynamics simulations (MDS): RMSD, RMSF, RG, SASA, MolSA, PSA and torsion angels

The molecular dynamics simulations provided insights into the dynamic behavior and stability of the protein-ligand complexes formed by the four bioactive compounds derived from *Bryophyllum pinnatum*. The RMSD values for the protein-ligand complexes ranged from 1.530682 Å to 2.111674 Å and individually for the ligands are ranges from 0.46445 Å to 0.699878 Å, indicating minimal structural deviation during the 100 ns simulation period (Fig. 10(**A–D**) and Fig. 11(**A–D**)). Notably, 4QNN-Bryophyllin A complex exhibited slightly higher RMSD value (2.111674 Å) compared to the other protein-ligand complexes, suggesting some degree of structural fluctuation. In terms of ligand stability, Bryophyllin A and B demonstrated the lowest RMSD value of 0.46445 Å and 0.475028 Å, indicating excellent structural preservation within the protein-ligand complex. Conversely, Bryotoxin A exhibited slightly higher RMSD value of 0.699878 Å, indicating relatively more significant structural deviations during the simulation.

The RMSF analysis provided insights into the flexibility of individual atoms within the ligands. Bryophyllin A displayed the lowest RMSF value of 0.48435 Å, indicating minimal atom-level fluctuation, while Bryophyllin B exhibited the highest RMSF value of 3.63705 Å, suggesting greater flexibility. Bryotoxin A and Bryotoxin B displayed intermediate RMSF values, indicating moderate flexibility of atoms within the ligands (Fig. 12(**A–D**)).

Regarding the radius of gyration (RG), Bryotoxin A exhibited the highest value of 5.792775 Å, indicating a larger spread of atoms from the center of mass, potentially reflecting a more extended conformation (Fig. 10D). In contrast, Bryophyllin B demonstrated the lowest RG value of 4.348928 Å, suggesting a more compact structure within the protein-ligand complex (Fig. 10A).

The solvent-accessible surface area (SASA) values provided insights into the accessibility of solvent molecules to the ligand surface. Bryophyllin A exhibited the lowest SASA value of 87.32623 $Å^2$, indicating relatively lower solvent exposure, while Bryotoxin B showed the highest SASA value of 310.6630 $Å^2$, indicating greater solvent accessibility (Fig. 10B and **C**).

Furthermore, the molecular surface area (MolSA) and polar surface area (PSA) values reflected the total surface area and the area occupied by polar atoms, respectively. Bryotoxin A exhibited the highest MolSA and PSA values, indicating a larger molecular surface area and a greater presence of polar atoms compared to the other compounds (Fig. 10(**A–D**)). These dynamic properties of the four

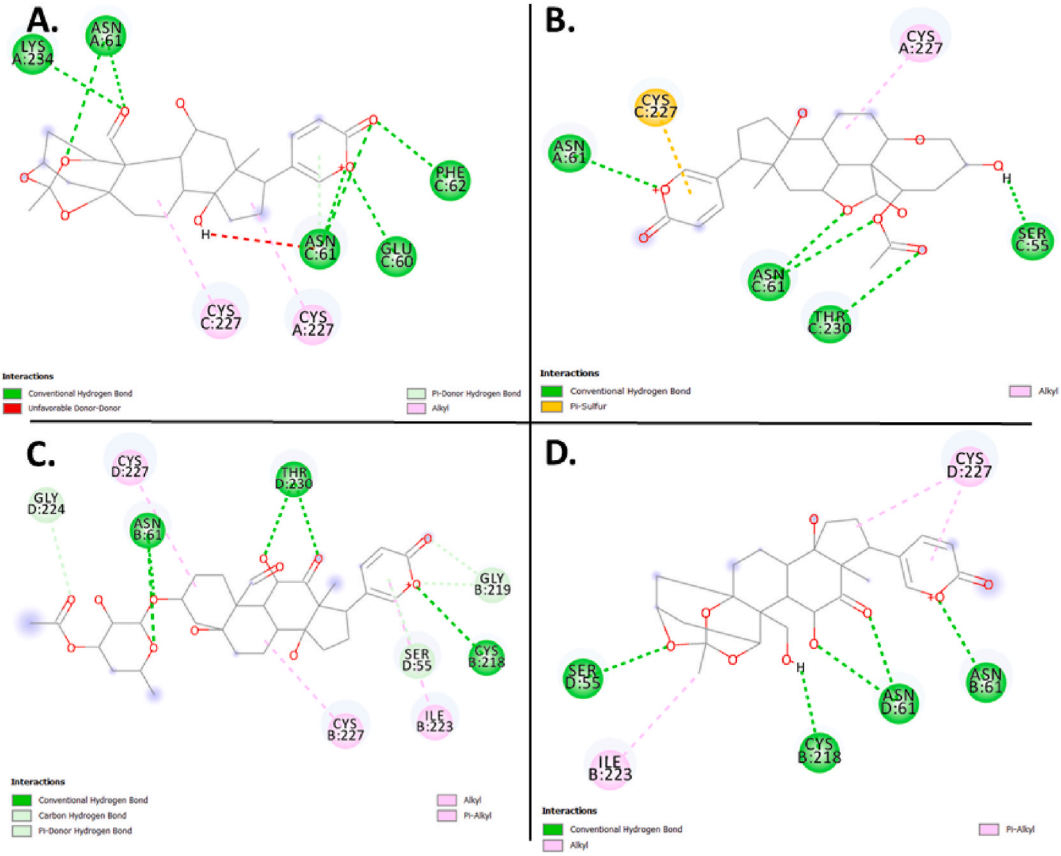

Fig. 9. Molecular docking: Binding interactions (Bond types) of the four bioactive compounds- **A.** Bryophyllin A, **B.** Bryophyllin B, **C.** Bryotoxin A, and **D.** Bryotoxin B from *Bryophyllum pinnatum* with the allergen protein Phospholipase A1 (Ves V1) of *Vespula vulgaris*.

Table 04
Molecule properties of the four bioactive compounds from *Bryophyllum pinnatum*.

Compounds	MW	LogP	RB	HBA	HBD	Surface Area	LOF Violations
Bryophyllin A	472.534	2.2512	2	8	2	197.117	0
Bryophyllin B	490.549	1.2056	2	9	4	202.598	0
Bryotoxin A	618.676	1.1374	5	12	4	254.224	2
Bryotoxin B	488.533	1.2236	2	9	3	201.911	0

Here, LOF: Lipinski rule of five.

Table 05
ADME analysis of the four bioactive compounds from *Bryophyllum pinnatum*.

Compounds	Absorption			Distribution		Metabolism	Excretion
	C2P	HIA (%)	P-gpI	BBB	CNS	CYP1A2	TC
				(Permeability)			
Bryophyllin A	1.351	85.237	No	−0.635	−3.077	No	0.254
Bryophyllin B	0.57	92.164	No	−0.973	−3.271	No	0.375
Bryotoxin A	0.616	56.276	Yes	−1.318	−3.32	No	0.373
Bryotoxin B	1.116	100	No	−0.896	−3.356	No	0.343

Here, TC = total clearance and measured in log mL/min/kg; I = inhibitor; Caco-2 permeability (C2P) (log Papp in 10^{-6} cm/s); human intestinal absorption (HIA) (% absorbed), and P-glycoprotein inhibitor (P-gpI); The blood-brain barrier (BBB) (log BB) and central nervous system (CNS) permeability (log PS).

Table 06
Toxicity analysis of the four bioactive compounds from *Bryophyllum pinnatum*.

Compounds	Oral Toxicity		Organ Toxicity	Toxicity Endpoints Prediction			
	Toxicity Class	Predicted LD50 (mg/kg)	Hepatotoxicity	Mutagenicity	Cyto Toxicity	Carcinogenicity	Immunotoxicity
Bryophyllin A	2	31	Inactive	Inactive	Active	Inactive	Active
Bryophyllin B	3	144	Inactive	Inactive	Active	Inactive	Active
Bryotoxin A	2	31	Inactive	Inactive	Active	Inactive	Active
Bryotoxin B	2	31	Inactive	Inactive	Inactive	Inactive	Active

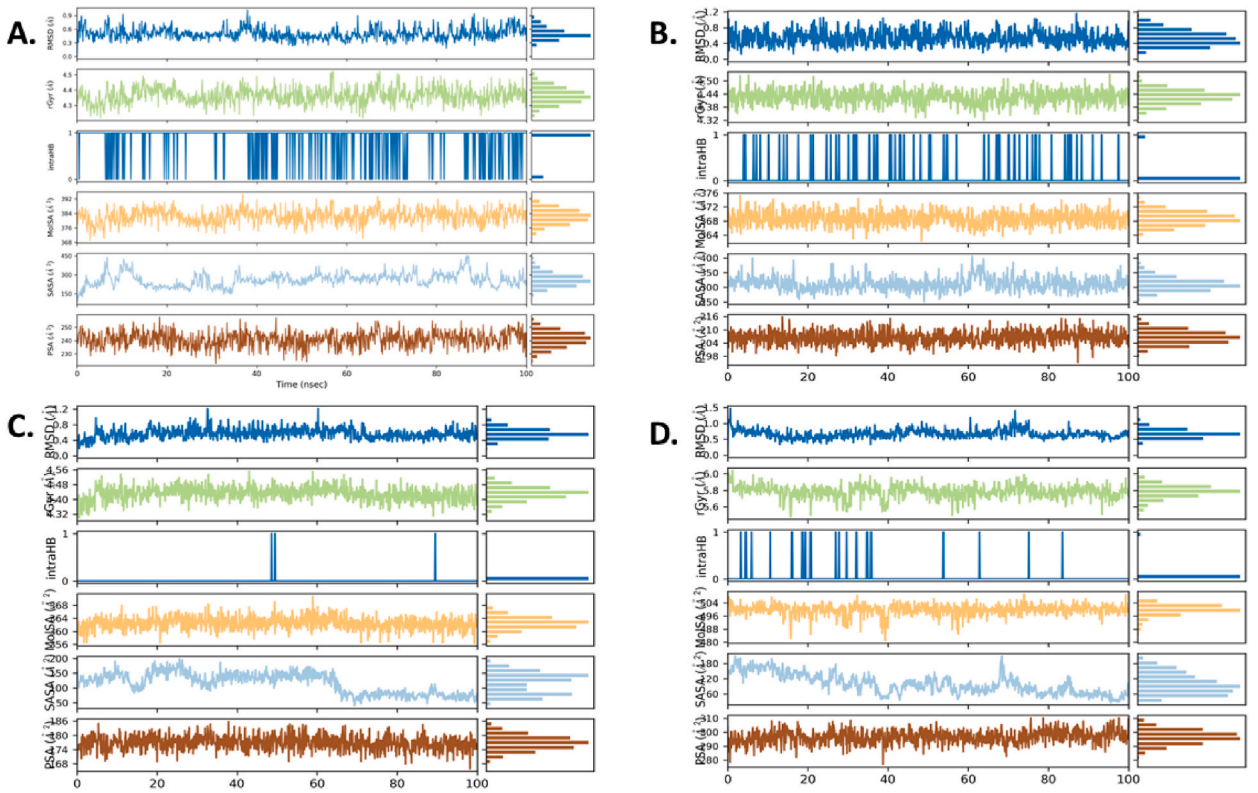

Fig. 10. Molecular Dynamics Simulations: Properties (PSA, SASA, MolSA, IntraHB, rGyr and RMSD) of the four bioactive compounds of *Bryophyllum pinnatum*: **(A)** Bryophyllin B, **(B)** Bryotoxin B, **(C)** Bryophyllin A, and **(D)** Bryotoxin A.

bioactive compounds are summarized in Table 07 which actually a short form of Table S2.

Understanding the dynamic behavior of amino acids and pinpointing specific modification sites within a protein are critical for interpreting functional dynamics during molecular dynamics simulations. The root mean square fluctuation (RMSF) analysis offers valuable insights into the variability of individual amino acids over the simulation trajectory. The average RMSF values for Bryophyllin B, Bryotoxin B, Bryophyllin A, and Bryotoxin A were determined for three allergen proteins: Antigen 5 (Ves V5, PDB: 1QNX), Hyaluronoglucosaminidase (Ves V2, PDB: 2ATM), and Phospholipase A1 (Ves V1, PDB: 4QNN). Notable fluctuations (1.4–3.8 Å) were observed in specific residues of Antigen 5, such as LYS_5, ILE_6, LYS_7, CYS_8, LEU_9, LYS_10, GLY_11, ASN_194, PHE_195, LYS_196, ASN_197, GLU_198, and GLU_199, particularly with Bryophyllin B (Fig. 13A). Here LEU_9 and LYS_10 formed alkyl bond and conventional hydrogen bond respectively with Bryophyllin B and these two amino acids showed moderate fluctuation of 3.706 Å and 2.548 Å respectively which denotes the flexibility the interactions.

For the allergen protein Hyaluronoglucosaminidase, residues including ASN_135, GLU_136, HIS_137, PRO_138, THR_139, TRP_140, ASN_141, LYS_142, and LYS_143 exhibited maximum fluctuations ranging from 2.1 to 9.8 Å (Fig. 13B). Similarly, for the allergen protein Phospholipase A1, residues like MET_91, SER_92, GLY_93, ILE_94, GLN_95, LEU_96, PRO_169, SER_170, PHE_171, LYS_172, SER_173, and ASN_174 showed fluctuations ranging from 2.5 to 7.5 Å with Bryotoxin B (Fig. 13C). Additionally, amino acid residues including ARG_18, GLU_19, ASN_20, LYS_21, LYS_22, HIS_23, ASP_24, GLU_89, GLU_90, MET_91, and others exhibited similar fluctuations with Bryotoxin A (Fig. 13D). Importantly, none of these highly fluctuating amino acid residues were directly involved in protein-ligand contacts. Despite the observed fluctuations, the protein-ligand complexes for all four compounds remained stable throughout the simulation. Notably, the allergen proteins Antigen 5, Hyaluronoglucosaminidase, and Phospholipase A1 demonstrated

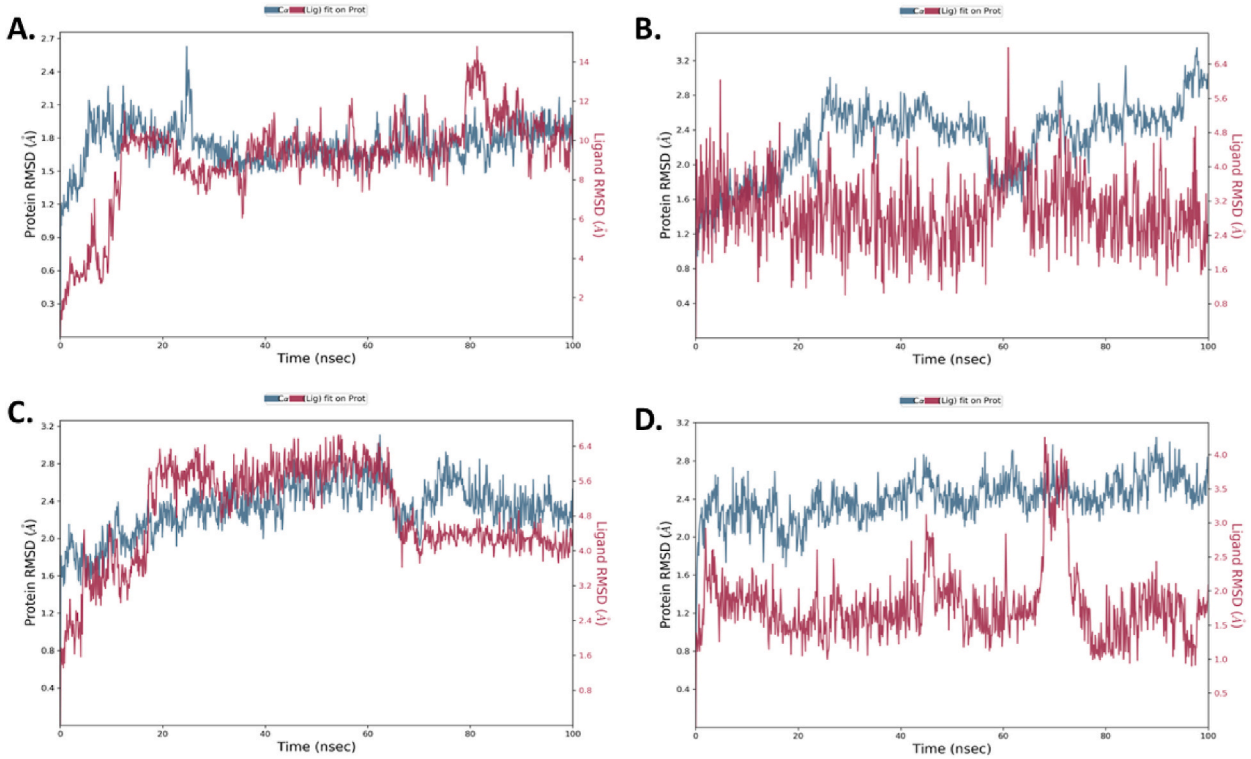

Fig. 11. Root Mean Square Deviation (RMSD) of protein-ligand complexes: **(A)** 1QNX-Bryophyllin B, **(B)** 2ATM-Bryotoxin B, **(C)** 4QNN-Bryophyllin A, and **(D)** 4QNN-Bryotoxin A.

enhanced stability, indicating robust interactions with the ligands.

The compounds are visually represented in a 2D schematic diagram, showcasing color-coded rotatable bonds (Fig. 14(A–D)). To provide a clearer understanding of these rotatable torsional bonds, a radial plot and corresponding color bar plots were introduced. The radial plot depicts the evolution of torsion angles over the simulation period, emanating from the center and extending outward with time. Bar plots accompanying the radial diagram summarize the probability density of torsion angles, with data expressed in kcal/mol on the Y-axis. This combined visualization method elucidates the relationship between torsion potential and conformational strain of the compounds while preserving their protein-bound conformation.

In summary, molecular dynamics simulations revealed distinct properties of the four bioactive compounds from *Bryophyllum pinnatum*. All compounds showed stable interactions within the protein-ligand complex, but differences in structural stability, flexibility, and surface properties were observed. These findings provide valuable insights for further investigation and development of these compounds as potential therapeutic agents.

3.5.1. Analysis of MDS: protein-ligand contacts

Based on the analysis of protein-ligand interactions during the 100ns molecular dynamics simulations, the interactions between the four bioactive compounds from *Bryophyllum pinnatum* and the respective allergen proteins of *V. vulgaris* were assessed, focusing on different types of interactions, including water bridges, hydrogen bonds, ionic interactions, and hydrophobic interactions.

For the protein-ligand complex Antigen 5 (Ves V5, PDB: 1QNX) with Bryophyllin B, a substantial number of interactions were observed, primarily dominated by water bridges (24 amino acid residues) and hydrogen bonds (10 amino acid residues). These interactions persisted for an average duration of 47 % and 8 % of the simulation period, respectively, indicating a notable engagement between Bryophyllin B and the Antigen 5 (Ves V5) protein (Fig. 15A). Among them, TYR_162 demonstrated hydrophobic interaction throughout the whole simulation period and PHE_151 for 40 % time period. Again, ASN_194 showed both H bond and water bridge interaction for 50 % time of simulation period. These long-time interactions denote the compact nature and strong stability of the protein-ligand contacts.

In the case of the protein-ligand complex Hyaluronoglucosaminidase (Ves V2, PDB: 2ATM) with Bryotoxin B, fewer interactions were observed compared to 1QNX-Bryophyllin B. However, hydrogen bonds were the predominant interaction type, involving 4 amino acid residues and persisting for 60 % of the simulation time. Water bridges and hydrophobic interactions were also present, albeit to a lesser extent (Fig. 15B). The amino acid residues TYR_67 and ASN_127 showed H bond interactions for 120 % and 60 % time of simulation time periods. PHE_128 showed hydrophobic interaction for 70 % time period which denote the strong binding stability with Bryotoxin B.

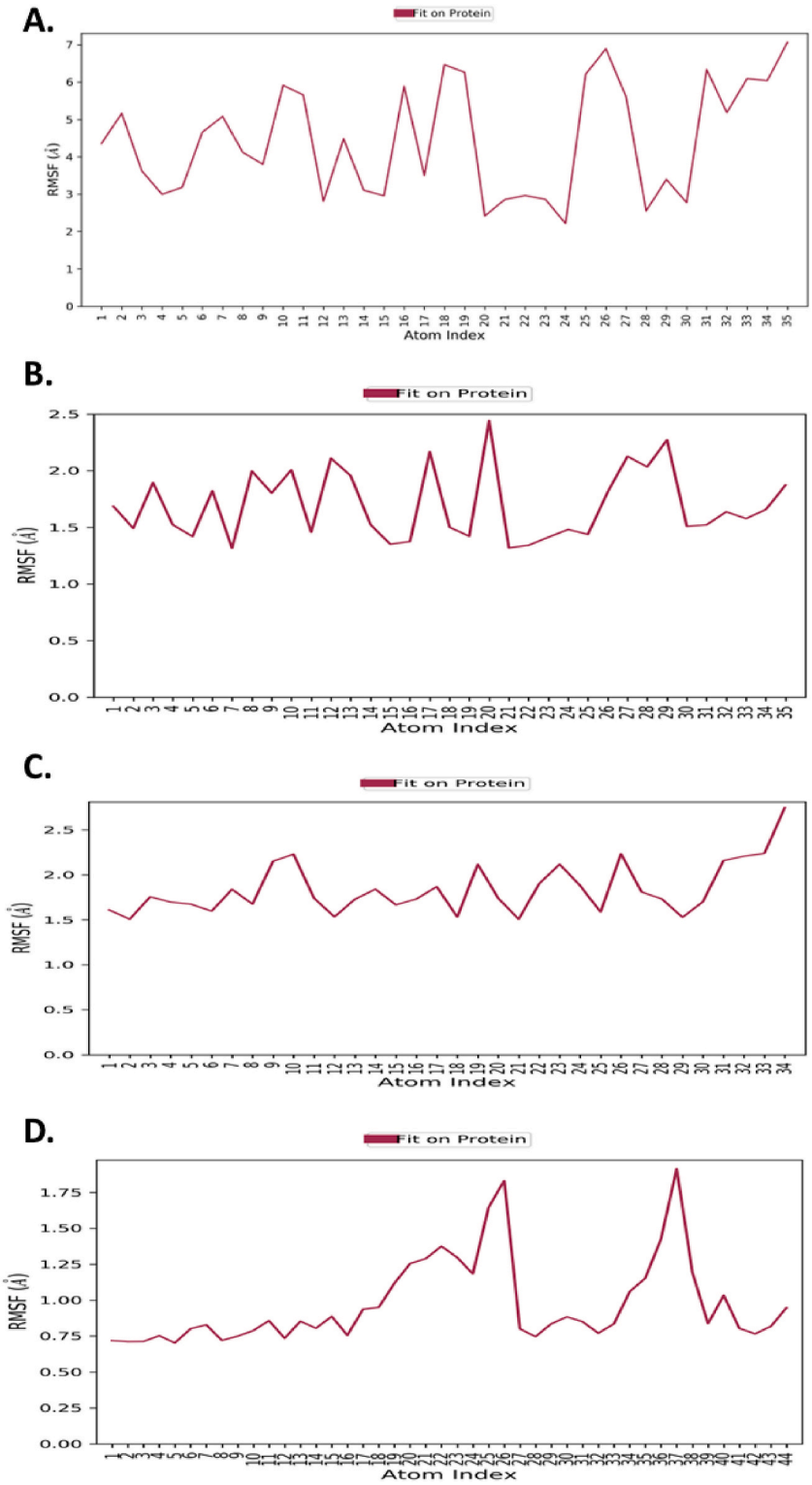

Fig. 12. Root Mean Square Fluctuation (RMSF) of the bioactive compounds- **(A)** Bryophyllin B, **(B)** Bryotoxin B, **(C)** Bryophyllin A, and **(D)** Bryotoxin A.

Table 07
Molecular Dynamics Simulations: The Summary of Properties of the top four compounds.

Ligand	Protein- ligand complex	Ligand					
	RMSD (Å)	RMSD (Å)	RMSF (Å)	RG (Å)	SASA (Å^2)	MolSA (Å^2)	PSA (Å^2)
Bryophyllin A	2.111674	0.46445	0.48435	4.41730	123.3923	361.1234	176.326
Bryophyllin B	1.613691	0.475028	3.63705	4.348928	201.2910	377.2109	243.1312
Bryotoxin A	1.617276	0.699878	0.5681	5.792775	87.32623	498.5362	294.2162
Bryotoxin B	1.530682	0.557712	1.8984	4.209431	310.6630	269.8755	206.4726

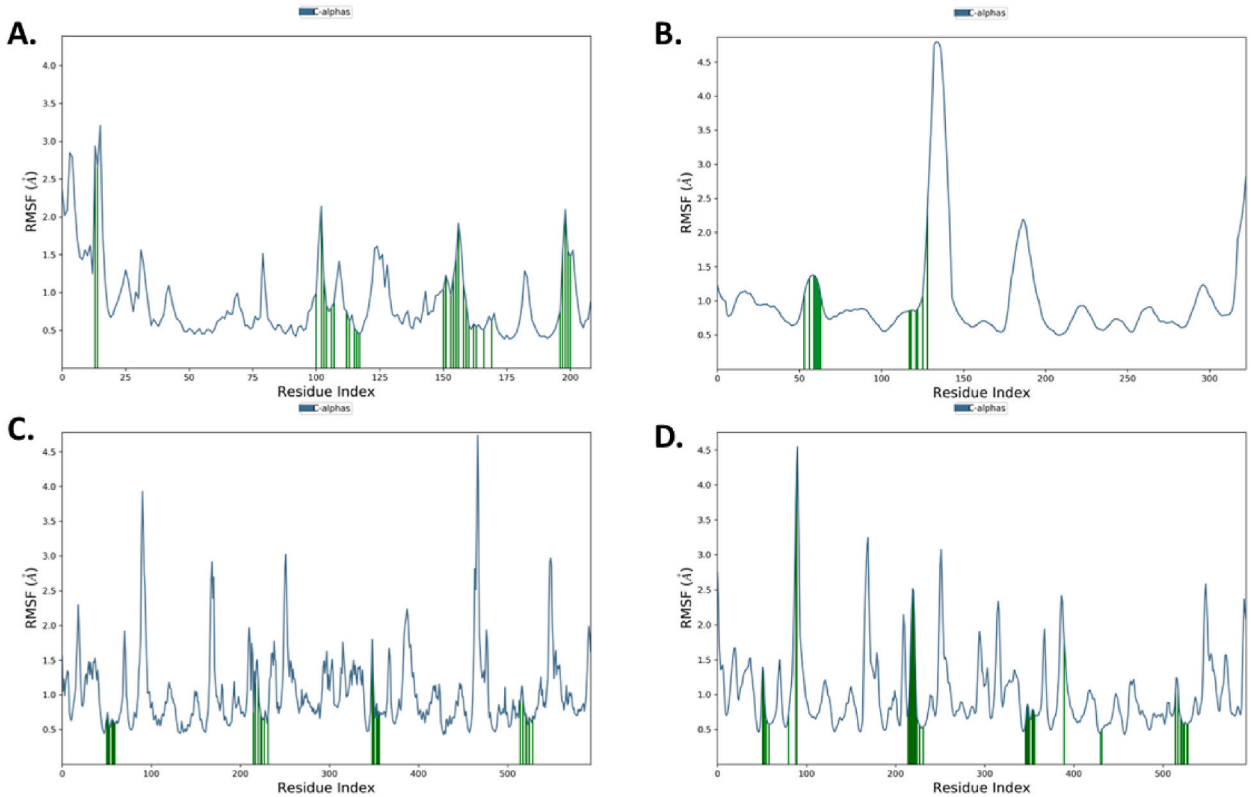

Fig. 13. Molecular Dynamics Simulation: RMSF plotting of allergen proteins- Antigen 5 (Ves V5, PDB: 1QNX), Hyaluronoglucosaminidase (Ves V2, PDB: 2ATM), and Phospholipase A1 (Ves V1, PDB: 4QNN) with **(A)** Bryophyllin B, **(B)** Bryotoxin B, **(C)** Bryophyllin A, and **(D)** Bryotoxin A respectively.

Moving to the protein-ligand complex Phospholipase A1 (Ves V1, PDB: 4QNN), both Bryophyllin A and Bryotoxin A exhibited significant interactions. Bryophyllin A formed water bridges with 24 amino acid residues, hydrogen bonds with 10 amino acid residues, and ionic interactions with 3 amino acid residues. These interactions persisted for 65 %, 34 %, and 2 % of the simulation time, respectively. Similarly, Bryotoxin A formed water bridges with 27 amino acid residues and hydrogen bonds with 12 amino acid residues, with durations of 70 % and 87 % of the simulation time, respectively (Fig. 15C and **D**). Both the amino acid residue B:THR_230 and D:LEU_220 exhibited H bond interaction for 65 % and 98 % of simulation time period. Again, B:THR_54, B:CYS_218, D:THR_54, D:SER_56, D:THR_59 and D:ASN_61 all exhibited water bridges interactions with Bryotoxin A for more than 40 % time of the simulation time period. A timeline representation of these protein-ligand contacts was supplemented on Figs. S1(A–D).

Overall, the interactions between the compounds and the allergen proteins varied in terms of types and durations. Bryophyllin B and Bryotoxin A exhibited extensive interactions with the Phospholipase A1 (Ves V1) protein, while Bryophyllin B displayed notable engagement with the Antigen 5 (Ves V5) protein. These findings suggest distinct binding modes and potential binding affinities of the compounds with their respective target proteins, providing valuable insights for further drug development efforts.

4. Discussion

Different analysis in this study provides valuable insights into the potential therapeutic efficacy and safety profiles of bioactive compounds derived from *Bryophyllum pinnatum* against allergen proteins from *V. vulgaris*. Through a comprehensive analysis

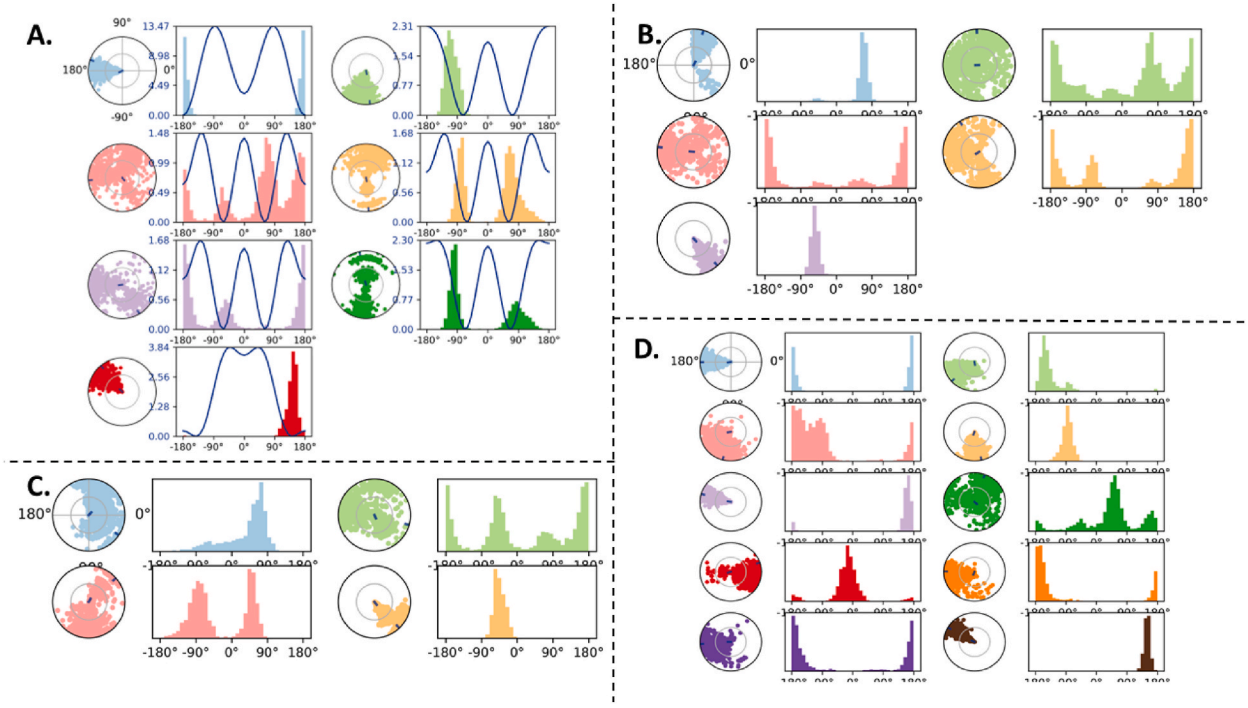

Fig. 14. Torsions of the four bioactive compounds- **(A)** Bryophyllin B, **(B)** Bryotoxin B, **(C)** Bryophyllin A, and **(D)** Bryotoxin A.

encompassing molecular docking, molecular properties assessment, and ADMET profiling, we have shed light on the promising candidates for inhibiting allergic reactions induced by wasp venom.

Firstly, the molecular docking analysis revealed robust binding interactions between the bioactive compounds and the allergen proteins, indicating strong potential for therapeutic intervention. Across all three proteins (Ves V1, Ves V2, and Ves V5), Bryophyllin B consistently exhibited high affinity (−9.6 kcal/mol), closely followed by Bryotoxin A (−10.0 kcal/mol), suggesting their strong binding capabilities with allergen proteins from *V. vulgaris*. The identified binding pockets were consistent among different proteins, suggesting potential shared interaction sites and highlighting the specificity of the compounds towards the target proteins.

Furthermore, the molecular properties analysis provided insights into the drug-likeness and pharmacokinetic characteristics of the compounds [51–54]. Bryophyllin A and Bryophyllin B demonstrated moderate molecular weights and favorable logP values, indicative of balanced hydrophilic-lipophilic profiles essential for efficient drug absorption and distribution. While Bryotoxin A and Bryotoxin B exhibited higher molecular weights and greater molecular flexibility, they still adhered to Lipinski's rule of five, albeit with a few violations, suggesting their potential as drug candidates.

The ADMET analysis further elucidated the pharmacokinetic properties and safety profiles of the compounds [48]. Bryophyllin B emerged as a promising candidate with high absorption, minimal metabolic interactions, and a low toxicity profile, making it a favorable choice for further development as a therapeutic agent. Importantly, all compounds exhibited favorable safety profiles in terms of hepatotoxicity, mutagenicity, and immunotoxicity, although cytotoxicity and carcinogenicity predictions warrant further investigation.

The analysis of molecular dynamics simulations (MDS) offers a comprehensive understanding of the dynamic behavior and stability of protein-ligand complexes formed by four bioactive compounds derived from *Bryophyllum pinnatum*. These simulations provide valuable insights into various parameters such as RMSD, RMSF, RG, SASA, MolSA, PSA, and torsion angles, shedding light on the structural dynamics and interactions within the complexes.

The RMSD values, indicative of structural deviation during the simulation period, ranged from 1.530682 Å to 2.111674 Å for the protein-ligand complexes, suggesting minimal structural changes. Notably, Bryophyllin A and B exhibited the lowest RMSD values for individual ligands, indicating excellent structural preservation within the complexes. Conversely, Bryotoxin A displayed slightly higher RMSD values, suggesting relatively more significant structural deviations [55–57].

The RMSF analysis provided insights into the flexibility of individual atoms within the ligands [58]. Bryophyllin A displayed minimal atom-level fluctuation, while Bryophyllin B exhibited greater flexibility. Bryotoxin A and B displayed intermediate flexibility, indicating moderate fluctuation of atoms within the ligands.

Regarding the radius of gyration (RG) [59], Bryotoxin A exhibited the highest value, suggesting a more extended conformation, while Bryophyllin B demonstrated the lowest RG value, indicating a more compact structure within the complexes.

Solvent-accessible surface area (SASA) values reflected the accessibility of solvent molecules to the ligand surface, with Bryophyllin A exhibiting relatively lower solvent exposure and Bryotoxin B showing greater solvent accessibility. Additionally, MolSA and PSA

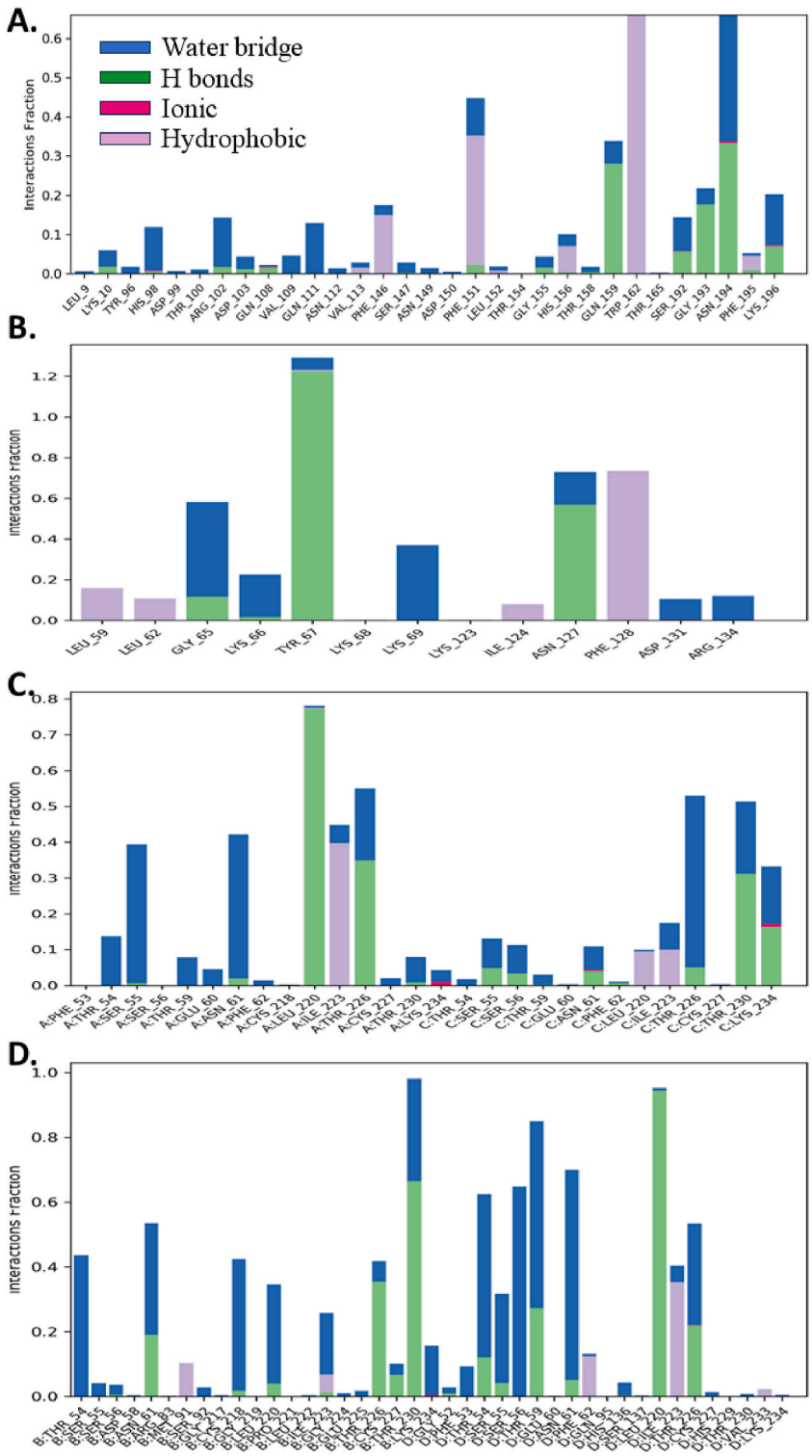

Fig. 15. Plot (stacked bar charts) of the bioactive compounds- **(A)** Bryophyllin B, **(B)** Bryotoxin B, **(C)** Bryophyllin A, and **(D)** Bryotoxin A interactions with the allergen proteins- Antigen 5 (Ves V5, PDB: 1QNX), Hyaluronoglucosaminidase (Ves V2, PDB: 2ATM), and Phospholipase A1 (Ves V1, PDB: 4QNN) of *Vespula vulgaris* supervised throughout the simulation period of 100ns.

values indicated differences in molecular surface area and the presence of polar atoms among the compounds.

The analysis of torsion angles provided further insights into the conformational dynamics of the compounds over the simulation period, elucidating their potential strain and stability within the protein-bound conformation.

Moreover, the analysis of protein-ligand contacts revealed extensive interactions between the compounds and allergen proteins, including water bridges, hydrogen bonds, and hydrophobic interactions. Each compound exhibited unique interaction profiles with the target proteins, indicating distinct binding modes and potential binding affinities.

Despite the observed fluctuations in dynamic properties, all protein-ligand complexes remained stable throughout the simulations, underscoring the robustness of their interactions. Notably, the allergen proteins demonstrated enhanced stability, further supporting the strong and stable binding affinity of the compounds.

In conclusion, this study highlights the potential of bioactive compounds from *Bryophyllum pinnatum* as inhibitors of *V. vulgaris* allergen proteins. Bryophyllin B, in particular, emerges as a most promising candidate with high binding affinity, favorable pharmacokinetic properties, a low toxicity profile and strong stability in protein-ligand complex. These findings pave the way for further research and development of novel therapeutics to mitigate the allergic burden imposed by wasp venom, emphasizing the importance of natural compounds in drug discovery and development.

5. Conclusion

In conclusion, this study unveiled *Bryophyllum pinnatum* compounds, particularly Bryophyllin B and Bryotoxin A as promising inhibitors for *V. vulgaris* allergen proteins. The strong binding affinities and favorable ADMET profiles make these compounds attractive candidates for further preclinical and clinical studies. The potential of Bryophyllin B as a lead compound emphasizes the importance of thorough drug development efforts. As we advance toward the goal of mitigating wasp venom allergies, these findings contribute valuable insights to the field, offering potential solutions to address the increasing prevalence of allergic reactions induced by *V. vulgaris* venom.

Data availability statement

Data included in article/supp. material/referenced in article.

CRediT authorship contribution statement

Sirajul Islam: Writing – original draft, Methodology, Data curation, Conceptualization. **Abu Zaffar Shibly:** Writing – review & editing, Visualization, Supervision, Data curation.

Declaration of competing interest

The authors declare that they have no known competing financial interests or personal relationships that could have appeared to influence the work reported in this paper.

Appendix A. Supplementary data

Supplementary data to this article can be found online at https://doi.org/10.1016/j.heliyon.2024.e34713.

References

[1] A. Henriksen, et al., Major venom allergen of yellow jackets, ves v 5: structural characterization of a pathogenesis-related protein superfamily, Proteins: Structure, Function and Genetics 45 (4) (Dec. 2001) 438–448, https://doi.org/10.1002/PROT.1160.

[2] A. Henriksen, et al., Major venom allergen of yellow jackets, ves v 5: structural characterization of a pathogenesis-related protein superfamily, Proteins: Structure, Function and Genetics 45 (4) (Dec. 2001) 438–448, https://doi.org/10.1002/PROT.1160.

[3] B. Bohle, B. Zwölfer, G. F.-… E. Allergy, and undefined, Characterization of the Human T Cell Response to Antigen 5 from Vespula Vulgaris (Ves V 5), Wiley Online Library, 2005 [Online]. Available: https://onlinelibrary.wiley.com/doi/abs/10.1111/j.1365-2222.2005.02180.x. (Accessed 19 March 2024).

[4] D. Kolarich, et al., A proteomic study of the major allergens from yellow jacket venoms, Proteomics 7 (10) (May 2007) 1615–1623, https://doi.org/10.1002/PMIC.200600800.

[5] B. Bohle, et al., Characterization of the human T cell response to antigen 5 from Vespula vulgaris (Ves v 5), Clin. Exp. Allergy 35 (3) (Mar. 2005) 367–373, https://doi.org/10.1111/J.1365-2222.2005.02180.X.

[6] R. Suck, B. Weber, H. Kahlert, S. H.-… archives of allergy and, and undefined, Purification and immunobiochemical characterization of folding variants of the recombinant major wasp allergen Ves v 5 (antigen 5) [Online]. Available: *karger.com*, 2000. (Accessed 19 March 2024) https://karger.com/iaa/article/121/4/284/164496.

[7] D. Kolarich, A. Loos, R. Léonard, L. M.-, and undefined, A Proteomic Study of the Major Allergens from Yellow Jacket Venoms, Wiley Online Library, Accessed, 2007 [Online]. Available: https://analyticalsciencejournals.onlinelibrary.wiley.com/doi/abs/10.1002/pmic.200600800. (Accessed 19 March 2024).

[8] A. Henriksen, T. King, O. M.-P. S., and undefined, Major Venom Allergen of Yellow Jackets, Ves V 5: Structural Characterization of a Pathogenesis-related Protein Superfamily, Wiley Online Library, 2001 [Online]. Available: https://onlinelibrary.wiley.com/doi/abs/10.1002/prot.1160. (Accessed 19 March 2024).

[9] S. Hofmann, N. Pfender, S. Weckesser, J. Huss-Marp, T. Jakob, Added value of IgE detection to rApi m 1 and rVes v 5 in patients with hymenoptera venom allergy, J. Allergy Clin. Immunol. 127 (2011).

[10] S. Blank, et al., Vitellogenins are new high molecular weight components and allergens (Api m 12 and Ves v 6) of apis mellifera and vespula vulgaris venom, PLoS One 8 (4) (Apr. 2013) e62009, https://doi.org/10.1371/JOURNAL.PONE.0062009.

[11] P. Korosec, R. Valenta, I. Mittermann, N. Celesnik, M. Silar, High sensitivity of CAP-FEIA rVes v 5 and rVes v 1 for diagnosis of vespula venom allergy, J. Allergy Clin. Immunol. 129 (2012).

[12] S. Hoffman, N. Pfender, S. Weckesser, S. Blank, J. Huss-Marp, Detection of IgE to a panel of species specific allergens further improves discrimination of bee and wasp venom allergy (Reply), J. Allergy Clin. Immunol. 128 (2011).

[13] M. Schiener, A. Graessel, M. Ollert, C.B. Schmidt-Weber, S. Blank, Allergen-specific immunotherapy of Hymenoptera venom allergy–also a matter of diagnosis, Hum Vaccin Immunother 13 (10) (Oct. 2017) 2467–2481, https://doi.org/10.1080/21645515.2017.1334745.

[14] B. Przybilla, F. Ruëff, Hymenoptera venom allergy, JDDG J. der Deutschen Dermatol. Gesellschaft 8 (2) (Feb. 2010) 114–129, https://doi.org/10.1111/J.1610-0387.2009.07125.X.

[15] B.M. Bilò, F. Bonifazi, Hymenoptera venom immunotherapy, Immunotherapy 3 (2) (Feb. 2011) 229–246, https://doi.org/10.2217/IMT.10.88.

[16] G.J. Sturm, et al., EAACI guidelines on allergen immunotherapy: hymenoptera venom allergy, Allergy: European Journal of Allergy and Clinical Immunology 73 (4) (Apr. 2018) 744–764, https://doi.org/10.1111/ALL.13262.

[17] I.J. Ansotegui, M. Sánchez-Borges, V. Cardona, Current trends in prevalence and mortality of anaphylaxis, Curr Treat Options Allergy 3 (3) (Sep. 2016) 205–211, https://doi.org/10.1007/S40521-016-0094-0.

[18] V. Cardona, et al., World allergy organization anaphylaxis guidance 2020, World Allergy Organization Journal 13 (10) (Oct. 2020) 100472, https://doi.org/10.1016/J.WAOJOU.2020.100472.

[19] P.J. Turner, D.E. Campbell, M.S. Motosue, R.L. Campbell, Global trends in anaphylaxis epidemiology and clinical implications, J. Allergy Clin. Immunol. Pract. 8 (4) (Apr. 2020) 1169–1176, https://doi.org/10.1016/J.JAIP.2019.11.027.

[20] M.A. Tejedor Alonso, M. Moro Moro, M.V. Múgica García, Epidemiology of anaphylaxis, Clin. Exp. Allergy 45 (6) (Jun. 2015) 1027–1039, https://doi.org/10.1111/CEA.12418.

[21] P.D. Bank, RCSB PDB: Homepage, Rcsb Pdb, 2019.

[22] M. Souza, H. S.-… of A. in, and undefined, An in silico analysis study of the chemical compounds from the crassulaceous plant Bryophyllum pinnatum (Lam.) oken against the SARS-COV-2 proteases [Online]. Available: *article.researchpromo.com*, 2023. (Accessed 19 March 2024) http://article.researchpromo.com/id/eprint/1771/.

[23] P. Rahman, M. Syaban, S. A.-… M. J. of, and undefined, Molecular docking analysis from Bryophyllum pinnatum Compound as A COVID-19 cytokine storm therapy [Online]. Available: https://oamjms.eu/index.php/mjms/article/view/8412, 2022. (Accessed 19 March 2024).

[24] P. Agrawal, G. B.-N. P. Communications, and undefined, Phytochemicals against SARS-COV-2 Infection, journals.sagepub.com, 2023 [Online]. Available: https://journals.sagepub.com/doi/abs/10.1177/1934578X231152168. (Accessed 19 March 2024).

[25] S. Dallakyan, A.J. Olson, Small-molecule library screening by docking with PyRx, Methods Mol. Biol. 1263 (2015) 243–250, https://doi.org/10.1007/978-1-4939-2269-7_19.

[26] D. Kitchen, H. Decornez, J. F.-N. reviews D., and undefined, Docking and scoring in virtual screening for drug discovery: methods and applications, in: nature.comDB Kitchen, H Decornez, JR Furr, J BajorathNature Reviews Drug Discovery, 2004•nature.Com, 2004, https://doi.org/10.1038/nrd1549.

[27] Y. Wang, et al., In silico ADME/T modelling for rational drug design, Q. Rev. Biophys. 48 (4) (Jul. 2015) 488–515, https://doi.org/10.1017/S0033583515000190.

[28] F. Rimmington, Pharmacokinetics and pharmacodynamics, South. Afr. J. Anaesth. Analg. 26 (6) (2020), https://doi.org/10.36303/SAJAA.2020.26.6.S3.2562.

[29] W.J. Egan, K.M. Merz, J.J. Baldwin, Prediction of drug absorption using multivariate statistics, J. Med. Chem. 43 (21) (Oct. 2000) 3867–3877, https://doi.org/10.1021/JM000292E.

[30] I. Muegge, Selection criteria for drug-like compounds, Med. Res. Rev. 23 (3) (May 2003) 302–321, https://doi.org/10.1002/MED.10041.

[31] A. Daina, O. Michielin, V. Zoete, SwissADME: a free web tool to evaluate pharmacokinetics, drug-likeness and medicinal chemistry friendliness of small molecules, Sci. Rep. 7 (Mar. 2017), https://doi.org/10.1038/SREP42717.

[32] S. Tian, J. Wang, Y. Li, D. Li, L. Xu, T. Hou, The application of in silico drug-likeness predictions in pharmaceutical research, Adv. Drug Deliv. Rev. 86 (2015), https://doi.org/10.1016/j.addr.2015.01.009.

[33] K. Lee, J. Jang, S. Seo, J. Lim, W.Y. Kim, Drug-likeness scoring based on unsupervised learning, Chem. Sci. 13 (2) (2022), https://doi.org/10.1039/d1sc05248a.

[34] C.Y. Jia, J.Y. Li, G.F. Hao, G.F. Yang, A drug-likeness toolbox facilitates ADMET study in drug discovery, Drug Discov. Today 25 (1) (2020), https://doi.org/10.1016/j.drudis.2019.10.014.

[35] J.B. Lee, et al., Quantitative analysis of lab-to-lab variability in Caco-2 permeability assays, Eur. J. Pharm. Biopharm. 114 (2017), https://doi.org/10.1016/j.ejpb.2016.12.027.

[36] Y. Li, et al., In vivo assessment of the effect of CYP1A2 inhibition and induction on pomalidomide pharmacokinetics in healthy subjects, J. Clin. Pharmacol. 58 (10) (2018), https://doi.org/10.1002/jcph.1145.

[37] P. Banerjee, A.O. Eckert, A.K. Schrey, R. Preissner, ProTox-II: a webserver for the prediction of toxicity of chemicals, Nucleic Acids Res. 46 (W1) (Jul. 2018) W257–W263, https://doi.org/10.1093/NAR/GKY318.

[38] A.S. Al Wasidi, A.S. Hassan, A.M. Naglah, In vitro cytotoxicity and druglikeness of pyrazolines and pyridines bearing benzofuran moiety, J Appl Pharm Sci 10 (4) (2020), https://doi.org/10.7324/JAPS.2020.104018.

[39] J.D. Durrant, J.A. McCammon, Molecular dynamics simulations and drug discovery, BMC Biol. 9 (2011), https://doi.org/10.1186/1741-7007-9-71.

[40] D.W. Borhani, D.E. Shaw, The future of molecular dynamics simulations in drug discovery, J. Comput. Aided Mol. Des. 26 (1) (2012), https://doi.org/10.1007/s10822-011-9517-y.

[41] M.R. Stalker, J. Grant, C.W. Yong, L.A. Ohene-Yeboah, T.J. Mays, S.C. Parker, Molecular simulation of hydrogen storage and transport in cellulose, Mol Simul 47 (2–3) (2021), https://doi.org/10.1080/08927022.2019.1593975.

[42] P.T. Kiss, A. Baranyai, Sources of the deficiencies in the popular SPCE and TIP3P models of water, J. Chem. Phys. 134 (5) (2011), https://doi.org/10.1063/1.3548869.

[43] K. Sargsyan, C. Grauffel, C. Lim, How molecular size impacts RMSD applications in molecular dynamics simulations, J Chem Theory Comput 13 (4) (Apr. 2017) 1518–1524, 10.1021/ACS.JCTC.7B00028/SUPPL_FILE/CT7B00028_SI_001.PDF.

[44] S.G. Hyberts, W. Märki, G. Wagner, Stereospecific assignments of side-chain protons and characterization of torsion angles in Eglin c, Eur. J. Biochem. 164 (3) (1987), https://doi.org/10.1111/j.1432-1033.1987.tb11173.x.

[45] S. K.-C. protocols and undefined, Exploring chemical information in PubChem, Wiley Online Library 1 (8) (Aug. 2021), https://doi.org/10.1002/cpz1.217, 2021.

[46] S. Kim, P. Thiessen, E. Bolton, J. C.-N. acids, and undefined, PubChem substance and compound databases [Online]. Available: https://academic.oup.com/nar/article-abstract/44/D1/D1202/2503131, 2016. (Accessed 19 March 2024).

[47] R. Halayal, Z. Bagewadi, N. A.-S. P., and undefined, Phytocompounds from Kalanchoe Pinnata in the Treatment of Diabetes Mellitus by Integrating Network Pharmacology, Molecular Docking and Simulation …, Elsevier, 2024 [Online]. Available: https://www.sciencedirect.com/science/article/pii/S1319016424000768. (Accessed 19 March 2024).

[48] G. Cruciani, Molecular interaction fields: applications in drug discovery and ADME prediction, Molecular Interaction Fields: Applications in Drug Discovery and ADME Prediction 27 (May 2006) 1–303, https://doi.org/10.1002/3527607676.

[49] V. Patel, R. Lalani, D. Bardoliwala, S. Ghosh, A. Misra, Lipid-based oral Formulation strategies for lipophilic drugs, AAPS PharmSciTech 19 (8) (Nov. 2018) 3609–3630, https://doi.org/10.1208/S12249-018-1188-8.

[50] V. Patel, R. Lalani, D. Bardoliwala, S. Ghosh, A.M.-A. Pharmscitech, undefined, Lipid-based Oral Formulation Strategies for Lipophilic Drugs, Springer, 2018 [Online]. Available: https://link.springer.com/article/10.1208/s12249-018-1188-8. (Accessed 19 March 2024).

[51] A. Ghatole, M. Gaidhane, K. L.-… : B. J. of, and undefined, Pharmacokinetics, drug-likeness, medicinal properties, molecular docking analysis of substituted β-lactams synthesized via -catalyzed, ceeol.com (2020) [Online]. Available: https://www.ceeol.com/search/article-detail?id=854964. (Accessed 20 March 2024).
[52] S. Udugade, R. Doijad, B. U.-J. of Advanced, and undefined 2019, In silico evaluation of pharmacokinetics, drug-likeness and medicinal chemistry friendliness of momordicin1: an active chemical constituent of momordica charantia, sciensage.info 10 (3) (2019) 222–229 [Online]. Available: http://www.sciensage.info/index.php/JASR/article/view/369. (Accessed 20 March 2024).
[53] M. Alam, J. Ahmed, D.L.-A.B. Chemistry, Biological Features, Drug-Likeness, Pharmacokinetic Properties, and Docking of 2-Arylidenehydrazinyl-4-Arylthiazole Analogues, Springer, and undefined 2016 [Online]. Available: https://link.springer.com/article/10.1007/s13765-016-0148-9. (Accessed 20 March 2024).
[54] M.S. Alam, J.U. Ahmed, D.U. Lee, Biological features, drug-likeness, pharmacokinetic properties, and docking of 2-arylidenehydrazinyl-4-arylthiazole analogues, Appl Biol Chem 59 (2) (Apr. 2016) 181–192, https://doi.org/10.1007/S13765-016-0148-9.
[55] J. Kirchmair, P. Markt, S. Distinto, G. Wolber, T. Langer, Evaluation of the performance of 3D virtual screening protocols: RMSD comparisons, enrichment assessments, and decoy selection - what can we learn from earlier mistakes? J. Comput. Aided Mol. Des. 22 (3–4) (2008) 213–228, https://doi.org/10.1007/S10822-007-9163-6.
[56] R. Brüschweiler, Efficient RMSD measures for the comparison of two molecular ensembles, Proteins: Structure, Function and Genetics 50 (1) (Jan. 2003) 26–34, https://doi.org/10.1002/PROT.10250.
[57] K. Sargsyan, C. Grauffel, C. Lim, How molecular size impacts RMSD applications in molecular dynamics simulations, J Chem Theory Comput 13 (4) (Apr. 2017) 1518–1524, https://doi.org/10.1021/ACS.JCTC.7B00028.
[58] A.M. Fonseca, B. Caluaco, J. Martinho, C. Madureira, Potential Inhibitors Targeting the Main Protease Structure of SARS-CoV-2 via Molecular Docking, and Approach with Molecular Dynamics, RMSD, RMSF, H-Bond, SASA …, Springer, 2023 https://doi.org/10.1007/s12033-023-00831-x.
[59] Y. Tamai, T. Konishi, Y. Einaga, M. Fujii, H. Yamakawa, Mean-square radius of gyration of oligo- and poly(methyl methacrylate)s in dilute solutions, Macromolecules 23 (18) (1990) 4067–4075, https://doi.org/10.1021/MA00220A007.